Volume 52 | Number 4 | 14 January 2016 | Pages 625–836

ChemComm

Chemical Communications

www.rsc.org/chemcomm

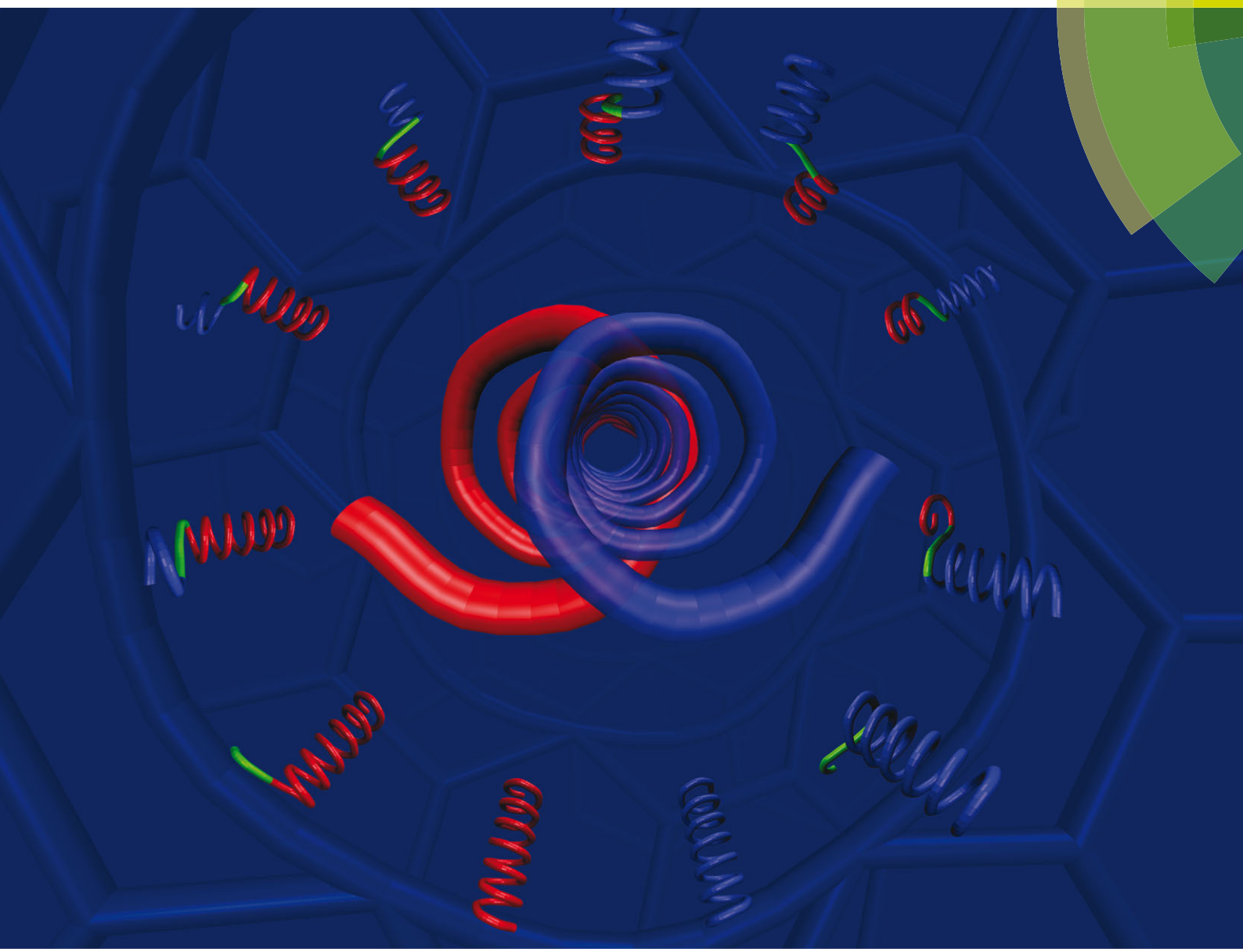

ISSN 1359-7345

ROYAL SOCIETY OF CHEMISTRY

COMMUNICATION

Vojislava Pophristic *et al.*

Helix handedness inversion in arylamide foldamers: elucidation and free energy profile of a hopping mechanism

175 YEARS

ChemComm

COMMUNICATION

View Article Online
View Journal | View Issue

Cite this: *Chem. Commun.*, 2016, 52, 669

Received 22nd August 2015,
Accepted 28th September 2015

DOI: 10.1039/c5cc07060k

www.rsc.org/chemcomm

Helix handedness inversion in arylamide foldamers: elucidation and free energy profile of a hopping mechanism†

Ara M. Abramyan, Zhiwei Liu and Vojislava Pophristic*

We report the first atomistic level description of the handedness inversion mechanism for helical arylamide foldamers. The key process in the handedness inversion is the simultaneous unfolding and folding of two adjacent aryl–aryl linkages, propagating from a helix terminus along the strand. Intermediates along the inversion pathway have a common feature – a single unfolded aryl–aryl linkage (through C_{aryl}–C_{amide} rotation) connecting two helical segments of opposite handedness. This explicit solvent metadynamics study also provides thorough quantitative free energy information for each step of the previously uncharacterized inversion pathway.

Chirality is a critical structural feature for a variety of chemical entities, with particularly prominent roles in folding and establishing the ultimate shape and function of natural and synthetic polymers. Consequently, the chirality of the ubiquitous helix motif has been an intriguing research topic in synthetic chemistry for decades.[1] Recent developments in computer technology and methodologies provide a currently under-utilized opportunity to build on the pioneering work of Green,[2] and reveal explicit, atomistic level information about the mechanisms and energetics of helix handedness inversion, which is inaccessible experimentally. A major challenge lies in the adaptation of computational tools originally developed for biopolymers. Here, we present the free-energy molecular dynamics (MD) elucidation of the handedness inversion mechanism for a representative of a large helical foldamer class. From both experimental and computational aspects, foldamers, non-natural oligomers that adopt a stable secondary structure in solution,[1b,3] are particularly attractive for the systematic studies of helix chirality.[4] This stems from their unlimited "helical codon" basis,[5] which allows for a high level of versatility and control over the resulting conformations.[4a,6]

Department of Chemistry & Biochemistry, University of the Sciences, 600 South 43rd Street, Philadelphia, PA 19104, USA. E-mail: v.pophri@usciences.edu; Fax: +1 215-596-8543

† Electronic supplementary information (ESI) available: Details of the simulation setup, quantum mechanical potential energy profiles of arylamide model compounds, additional FEPs (end-to-end distance as one of the CVs, different solvents), error analysis. See DOI: 10.1039/c5cc07060k

The handedness of helical foldamers, in particular arylamide-based ones, has therefore been a subject of a focused and fast-expanding experimental exploration in the past decade.[4b,7] This effort has, however, not been accompanied by a complementary computational activity, as it requires suitable force field optimizations, a task our group has undertaken recently.[8]

Free-energy MD methods are of particular interest for exploring the handedness inversion mechanism, because they can yield detailed reaction pathways and associated energetics.[9] However, they have been only scarcely used to study these problems.[10] The main obstacle in applying these methods to complex systems is the practical limitation of up to only two to three collective variables (CVs), which have to be chosen to drive the free energy surface exploration in the direction of a targeted reaction path, *i.e.* the process outcome.[11] We designed our CVs to be inherently related to the helix secondary structure and backbone conformation. Thus, our CVs have a direct and clearly defined relationship with the geometrical variables that drive the folding/unfolding process at the primary structure (*i.e.* sequence) level. The resulting reaction path and energetics thus reveal specific backbone torsions that are responsible for helix handedness inversion. Furthermore, for the arylamide systems, relatively short helices are representative of longer helices, allowing for information transferability and generality of our conclusions.[8c] Finally, our endeavour involves recently optimized parameters, necessary for the accurate MD simulations of arylamide foldamers.[8c,g]

Using this approach, we have deciphered and now report the hopping mechanism of arylamide helix inversion.[7i] This study reveals, for the first time, an atomistic level insight into the structure of the inversion center, backbone internal bond rotations that drive the propagation mechanism, and their cooperation. In particular, we show how helix handedness reversal propagates through the simultaneous unfolding of one monomer–monomer linkage and refolding of the adjacent one.

In this work, we focus on helical arylamides derived from 8-amino-2-quinolinecarboxilic acid because of their remarkable stability and consequent availability of extensive experimental information,[7g,i,j,12] including conformational characterization

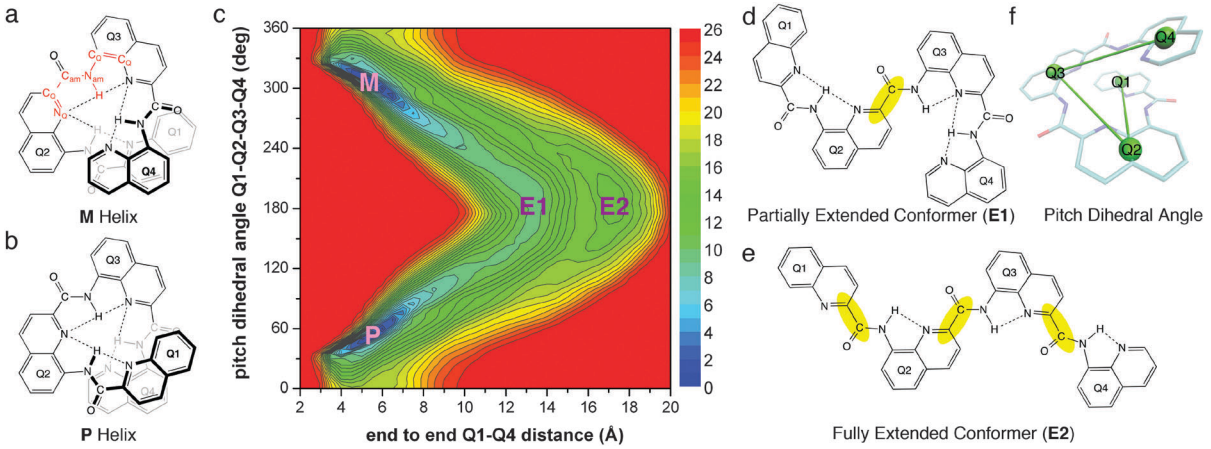

Fig. 1 (a and b) Structures of the left (*M*) and right (*P*) handed quinoline based tetramer helices. The N_Q–C_Q–C_{am}–N_{am} and C_Q–C_Q–N_{am}–H dihedral angles are shown in red. Dotted lines indicate H-bonds; (c) free energy profile (kcal mol^{-1}); (d and e) structures of the partially and fully extended conformers. Highlighted in yellow are the bonds that rotated ~180°; and (f) pitch dihedral angle.

in solution and kinetic data on handedness inversion. Using various experimental techniques, Huc and coworkers determined the kinetic rate constants and free energy barriers for racemization of these oligomers ranging from a hexamer to a hexadecamer at different temperatures.[7i] The results led to the hypothesis that the oligomers do not fully unfold during handedness inversion; instead, a hopping mechanism was suggested in which a local inversion center, separating two helical segments of opposite handedness, propagates along the strand from one end to the other. The general features of the mechanism have been supported for related systems.[2,5,13]

Utilizing force field parameters specifically optimized for the quinoline based arylamides (Fig. 1), we carried out all-atom MD simulations (300–500 ns) in explicit solvents (chloroform and water), combined with the metadynamics free-energy method,[9] on tetramer, pentamer and hexamer helices. This method accelerates the simulation by adding small repulsive potentials ("hills") to the underlying free energy landscape, thus gradually biasing the system to escape energy minima and explore the wide conformational space. From metadynamics simulations, we determined the free energy of the three oligomers with respect to two CVs to generate two-dimensional free energy profiles (FEPs). At least one CV in each metadynamics simulation is chosen to be a pitch dihedral angle. This angle (Fig. 1f), defined by the centers of masses (COMs) of four consecutive quinoline rings ("Q"), identifies the handedness of the helix: a positive dihedral angle for right-handed (*P*) and a negative angle for left-handed (*M*) helices. Here, we focus on our findings in chloroform, as the discussed mechanism remains the same in both solvents.

Fig. 1c shows the FEP for the handedness inversion of a tetramer, which has close to 1.5 turns and one pitch dihedral angle (∠Q1–Q2–Q3–Q4, Fig. 1f). The handedness inversion does not require the tetramer to extend fully (*i.e.* to turn into **E2**, Fig. 1e); the more energetically accessible inversion path goes *via* an end-to-end distance of only ~13 Å and a barrier of ~9.5 kcal mol^{-1} (through the partially extended **E1** conformer, Fig. 1d).

At the atomistic level, the *P* and *M* helices differ in the distribution of the backbone dihedral angles N_Q–C_Q–C_{am}–N_{am} and C_Q–C_Q–N_{am}–H (Fig. 1a and 2). In both *P* and *M* helices, the atomistic dihedral angles are close to 0°, indicating an intramolecular hydrogen-bond (H-bond) between the endocyclic N_Q and the amide proton. The inversion of the handedness requires a slight positive to negative (or *vice versa*) shift of the atomistic dihedral angle. In principle, this can occur either through 0°, which is energetically effortless, or through 180°, which requires breaking of the intramolecular H-bond and conjugation (Fig. S1, ESI†).

In helical oligomers, however, steric clashes between stacked aromatic units (*e.g.* Fig. 1a, b and f, Q1 and Q4) make the rotation of C_Q–C_{am} or C_Q–N_{am} through 0° improbable. The handedness inversion of tetramer, therefore, occurs *via* **E1** with ∠Q1–Q2–Q3–Q4 = 180° (Fig. 1c and d). It should be noted that the inversion of Q2–amide–Q3 requires only one of the two aryl–amide bonds (C_{Q2}–C_{am} or C_{Q3}–N_{am}) to rotate to 180°. The detailed conformational analysis of **E1** indicates that the 180° rotation occurs exclusively around the C_{Q2}–C_{am} bond (highlighted in yellow, Fig. 1d), whereas the N_{am}–C_{Q3} linkage maintains the H-bonded conformation. This is consistent with our quantum mechanical results (Fig. S1, ESI†).

The 180° rotation of the C_{Q2}–C_{am} bond opens up the stacked aromatic units Q1 and Q4 (Fig. 1d). Therefore, from the

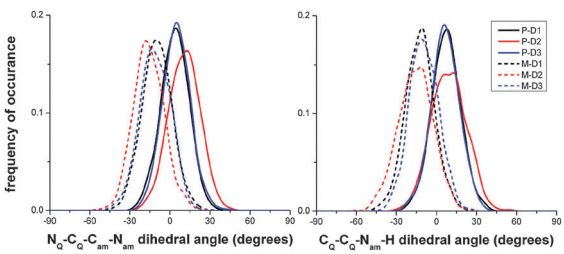

Fig. 2 The distribution of the atomistic N_Q–C_Q–C_{am}–N_{am} and C_Q–C_Q–N_{am}–H dihedral angles in the *M* and *P* helical conformers collected from the 300 ns simulation of tetramer in chloroform. D1, D2 and D3 denote atomistic dihedral angles between Q1 and Q2, Q2 and Q3, and Q3 and Q4 (Fig. 1), respectively.

intermediate **E1**, no additional 180° rotations are necessary for the remaining five aryl–amide torsions (two pairs at the termini and N_{am}–C_{Q3}) for the tetramer to invert its handedness. The torsions now can easily adjust from slightly positive to slightly negative values (or *vice versa*) through 0° while maintaining the intramolecular H-bonds. As evidenced by Fig. 1c, the fully extended conformer (**E2**), in which both C_{Q1}–C_{am} and C_{Q3}–C_{am} rotate by 180°, is higher in energy and is not a necessary state for the handedness inversion of tetramer.

For both pentamer and hexamer, metadynamics simulations using end-to-end distance as a CV (Fig. S2, ESI†) demonstrate that their handedness inversion also goes through partially extended intermediates. Fig. 3 shows the FEP of pentamer handedness inversion as a function of its two pitch dihedral angles. We labelled the minima and intermediates based on the states of the two central aryl–aryl linkages, *i.e.* the two corresponding pitch dihedral angles. The "**R**" (right) state corresponds to a pitch dihedral angle centered at ~60°, "**E**" (extended) to ~180° and "**L**" (left) to ~300°. There are two global minima, **RR** (*P*) and **LL** (*M*), and two inversion pathways involving the **RE** and **EL** local minima in one (Fig. 3, upper left), and **ER** and **LE** in the other case (Fig. 3, lower right). Each local minimum has one extended (**E**) and one folded (**L** or **R**) aryl–aryl linkage and lies ~8.3 kcal mol^{-1} (**RE**, **EL**) or ~9.3 kcal mol^{-1} (**ER**, **LE**) above the global minima. The **RR** ↔ **RE** ↔ **EL** ↔ **LL** pathway features transition states with energies of ~11.5, ~15.0 and ~12.0 kcal mol^{-1}. The **RR** ↔ **ER** ↔ **LE** ↔ **LL** pathway (Fig. 4) has transition states at ~12.0, ~16.0 and ~12.3 kcal mol^{-1}. A ~1 kcal mol^{-1} difference between the two pathways (above the FEP's estimated error of ~0.55 kcal mol^{-1}, Fig. S6, ESI†), stems from the N to C asymmetry of the helix and is also observed in the hexamer FEP (see below). An inversion from the N-terminus thus slightly differs from an inversion from the C-terminus. Clearly, both pathways (**RR** ↔ **RE** ↔ **EL** ↔ **LL** and **RR** ↔ **ER** ↔ **LE** ↔ **LL**) follow the general mechanism in which the helix undergoes local inversion that starts at one end and propagates to the other. The most important finding about the pentamer inversion pathway lies

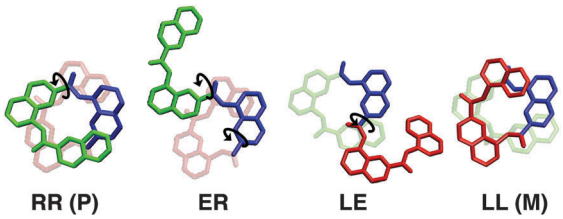

Fig. 4 Snapshots from the metadynamics simulation of the pentamer, showing the handedness inversion mechanism and characteristic conformers on the **RR** ↔ **ER** ↔ **LE** ↔ **LL** path.

in the **RE** ↔ **EL** and **ER** ↔ **LE** transition steps, *i.e.* simultaneous folding of one aryl–aryl linkage while its neighbouring aryl–aryl linkage unfolds (Fig. 4). Finally, at the atomistic level, similarly to the tetramer, the **R** → **E** and **L** → **E** transitions are almost exclusively achieved by the 180° rotation of the C_Q–C_{am} bonds.

Fig. 5 shows the FEP for the hexamer handedness inversion as a function of its pitch dihedral angles Q1–Q2–Q3–Q4 (N-terminal) and Q3–Q4–Q5–Q6 (C-terminal). The energy difference between the two global minima (**RRR** (*P*) and **LLL** (*M*)) is less than 0.1 kcal mol^{-1}, indicating sufficient conformational sampling. In order to reveal information about the middle pitch dihedral angle Q2–Q3–Q4–Q5, we extracted the conformations from each minimum basin (1–2 kcal mol^{-1} around the minimum), from the 500 ns MD trajectory. These conformations were analyzed and labelled using **R**, **E**, and **L** based on the folded *vs.* unfolded states of the three aryl–aryl linkages associated with the three pitch dihedral angles.

There are seven local minima, each corresponding to a state where only one aryl–aryl linkage is unfolded. In the case of the **LER**/**REL** minima, both **L** and **R** components are present. Furthermore, there are two **LER** minima (Fig. 5), one reached *via* C_{Q3}–C_{am} 180° rotation (lower in energy), the other *via* C_{Q4}–N_{am} 180° rotation. Similarly to the pentamer, the unwinding starts at one end of a global minimum conformer (**RRR** or **LLL**). As the pitch dihedral angle Q1–Q2–Q3–Q4 or Q3–Q4–Q5–Q6 unfolds and overcomes a ~11–12 kcal mol^{-1} barrier, the conformer converts to

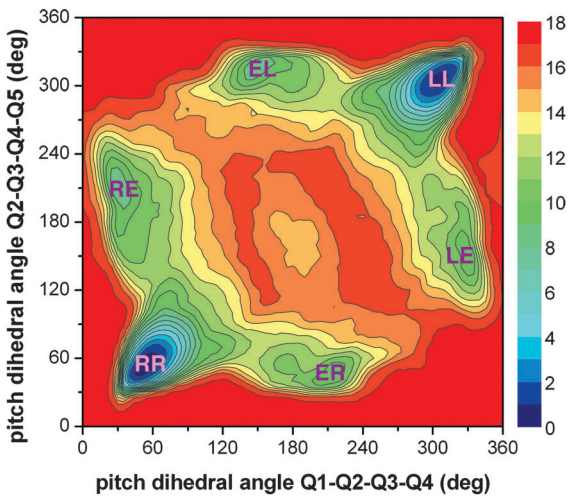

Fig. 3 Pentamer free energy profile (energy in kcal mol^{-1}) in chloroform. Note that **LL** and **RR** correspond to *M* and *P*, respectively.

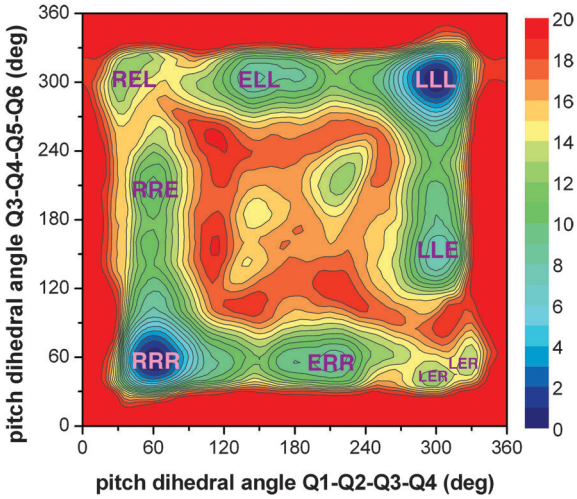

Fig. 5 Hexamer free energy profile (energy in kcal mol^{-1}) in chloroform. Note that **LLL** and **RRR** correspond to *M* and *P*, respectively.

ERR (or **RRE**) if started from **RRR**, or **ELL** (or **LLE**) if started from **LLL**. These states have an elevated energy of ~7–10 kcal mol^{-1}. The local inversion center (the **E** state) then propagates to the next pitch dihedral angle (the central Q3–Q4 linkage), whereas the previously unfolded pitch dihedral angle folds to the inverted state. These propagations, *i.e.* the **ER**R↔**LE**R, R**RE**↔R**EL**, **EL**L↔**RE**L and L**LE**↔L**ER** transitions, are essentially the same as those observed in the pentamer (**RE** ↔ **EL** and **ER** ↔ **LE**). This process of simultaneous folding and unfolding of the adjacent aryl–aryl linkages has a barrier of ~16–17 kcal mol^{-1}. The resulting **LER** and **REL** states are at ~12–13 kcal mol^{-1} and have opposite handedness on the two sides of the unfolded linkage. This leads to the two inversion pathways: **RRR** ↔ **RRE** ↔ **REL** ↔ **ELL** ↔ **LLL** and **RRR** ↔ **ERR** ↔ **LER** ↔ **LLE** ↔ **LLL**. Finally, as in the pentamer case, the asymmetry of the helix results in the first pathway being slightly more energetically favorable.

The highest energy barrier of ~16–17 kcal mol^{-1} for the hexamer handedness inversion (at 300 K) agrees with the experimentally measured Gibbs activation energy of 20.6 kcal mol^{-1} at 283 K.[7i] The difference comes from the fact that, in the experiments, 4-quinoline isobutoxyl groups are attached to the outer rim of the helix, adding extra steric hindrance to the helix inversion and thus increasing its barrier. In addition, the different temperature and solvents used (chloroform *vs.* chloroform/hexane) might contribute to the discrepancy. Indeed, a solvent-dependency study[12] has shown that both highly non-polar and protic polar solvents enhance the stability of the quinolone-based helices. Our metadynamics simulations in water (ESI†) show an increase in inversion barriers with respect to chloroform, due to the solvophobic stabilization of the folded structure. Importantly, in our simulations, the increase of the highest barrier on the inversion pathway from the pentamer to the hexamer is ~1 kcal mol^{-1}, in parallel with the experimentally observed <1 kcal mol^{-1} increase associated with the growth of oligomer by one unit in the hexamer to hexadecamer series.[7i] Finally, our results directly confirm the previously postulated hopping mechanism[2,5,7i,13a] and translate these "coarse grained" models to explicit backbone bond rotations.

In conclusion, we identified atomistic level motions that govern a stepwise unfolding–folding pathway for helical arylamides (Fig. 4), and determined associated free-energy profiles. The initial step of the hopping mechanism is the unwinding of the 2nd (or 2nd to the last) aryl–aryl linkage, almost exclusively *via* the C_Q–C_{am} 180° rotation, to form an intermediate with a single unfolded aryl–aryl linkage. The inversion is then followed by successive propagation steps; in each step, the unfolded linkage folds into the opposite handedness accompanied by simultaneous unwinding of the next aryl–aryl linkage. The process can be generalized as follows: $\mathbf{R}_n \leftrightarrow \mathbf{R}_{n-1}\mathbf{E} \leftrightarrow \mathbf{R}_{n-2}\mathbf{EL}\cdots\mathbf{R}_{n-m}\mathbf{EL}_{m-1}\cdots\mathbf{REL}_{n-2} \leftrightarrow \mathbf{EL}_{n-1} \leftrightarrow \mathbf{L}_n$, where n is the total number of pitch dihedral angles (number of monomers in the oligomer minus 3) and m is the step in the conversion from **R** to **L** helix. This mechanism involves the breakage of the fewest H-bonds and the minimal disturbance of aromatic stacking. A longer oligomer has to go through more steps to completely inverse its handedness; however, the energy barrier at each step is not significantly affected by the length of the oligomer, in agreement with experimental measurements.[7i] Studies on the energetics and mechanism of handedness control by the addition of a chiral biasing group on folding/unfolding of helical arylamide foldamers are underway.

This research was supported by the NSF grants MSN-1049771 and MRI CHE-1229564.

Notes and references

1 (*a*) J. Cornelissen, A. E. Rowan, R. J. M. Nolte and N. Sommerdijk, *Chem. Rev.*, 2001, **101**, 4039; (*b*) D. J. Hill, M. J. Mio, R. B. Prince, T. S. Hughes and J. S. Moore, *Chem. Rev.*, 2001, **101**, 3893; (*c*) T. Nakano and Y. Okamoto, *Chem. Rev.*, 2001, **101**, 4013; (*d*) E. Yashima, K. Maeda, H. Iida, Y. Furusho and K. Nagai, *Chem. Rev.*, 2009, **109**, 6102.
2 (*a*) M. M. Green, J. W. Park, T. Sato, A. Teramoto, S. Lifson, R. L. B. Selinger and J. V. Selinger, *Angew. Chem., Int. Ed.*, 1999, **38**, 3139; (*b*) S. Lifson, C. E. Felder and M. M. Green, *Macromolecules*, 1992, **25**, 4142.
3 (*a*) S. H. Gellman, *Acc. Chem. Res.*, 1998, **31**, 173; (*b*) K. C. M. Goodman, S. Choi, S. Shandler and W. F. DeGrado, *Nat. Chem. Biol.*, 2007, **3**, 252.
4 (*a*) *Foldamers: Structure, Properties, and Applications*, ed. S. Hecht and I. Huc, Wiley-VCH, Weinheim, 2007; (*b*) D.-W. Zhang, X. Zhao, J.-L. Hou and Z.-T. Li, *Chem. Rev.*, 2012, **112**, 5271.
5 M. Ohkita, J. M. Lehn, G. Baum and D. Fenske, *Chem. – Eur. J.*, 1999, **5**, 3471.
6 (*a*) G. Guichard and I. Huc, *Chem. Commun.*, 2011, **47**, 5933; (*b*) B. Gong, *Acc. Chem. Res.*, 2008, **41**, 1376.
7 (*a*) I. Saraogi and A. D. Hamilton, *Chem. Soc. Rev.*, 2009, **38**, 1726; (*b*) R. A. Brown, V. Diemer, S. J. Webb and J. Clayden, *Nat. Chem.*, 2013, **5**, 853; (*c*) J. Maury, B. A. F. Le Bailly, J. Raftery and J. Clayden, *Chem. Commun.*, 2015, **51**, 11802; (*d*) L. Byrne, J. Sola, T. Boddaert, T. Marcelli, R. W. Adams, G. A. Morris and J. Clayden, *Angew. Chem., Int. Ed.*, 2014, **53**, 151; (*e*) R. W. Sinkeldam, M. H. C. J. van Houtem, K. Pieterse, J. A. J. M. Vekemans and E. W. Meijer, *Chem. – Eur. J.*, 2006, **12**, 6129; (*f*) V. Maurizot, C. Dolain and I. Huc, *Eur. J. Org. Chem.*, 2005, 1293; (*g*) C. Dolain, H. Jiang, J. M. Leger, P. Guionneau and I. Huc, *J. Am. Chem. Soc.*, 2005, **127**, 12943; (*h*) C. Dolain, J. M. Leger, N. Delsuc, H. Gornitzka and I. Huc, *Proc. Natl. Acad. Sci. U. S. A.*, 2005, **102**, 16146; (*i*) N. Delsuc, T. Kawanami, J. Lefeuvre, A. Shundo, H. Ihara, M. Takafuji and I. Huc, *ChemPhysChem*, 2008, **9**, 1882; (*j*) A. M. Kendhale, L. Poniman, Z. Dong, K. Laxmi-Reddy, B. Kauffmann, Y. Ferrand and I. Huc, *J. Org. Chem.*, 2011, **76**, 195; (*k*) N. Delsuc, S. Massip, J.-M. Leger, B. Kauffmann and I. Huc, *J. Am. Chem. Soc.*, 2011, **133**, 3165; (*l*) S. J. Dawson, A. Meszaros, L. Petho, C. Colombo, M. Csekei, A. Kotschy and I. Huc, *Eur. J. Org. Chem.*, 2014, 4265; (*m*) J. L. Hou, H. P. Yi, X. B. Shao, C. Li, Z. Q. Wu, X. K. Jiang, L. Z. Wu, C. H. Tung and Z. T. Li, *Angew. Chem., Int. Ed.*, 2006, **45**, 796.
8 (*a*) J. F. Galan, J. Brown, J. L. Wildin, Z. Liu, D. Liu, G. Moyna and V. Pophristic, *J. Phys. Chem. B*, 2009, **113**, 12809; (*b*) J. F. Galan, C. N. Tang, S. Chakrabarty, Z. Liu, G. Moyna and V. Pophristic, *Phys. Chem. Chem. Phys.*, 2013, **15**, 11883; (*c*) Z. Liu, A. M. Abramyan and V. Pophristic, *New J. Chem.*, 2015, **39**, 3229; (*d*) Z. Liu, R. C. Remsing, D. Liu, G. Moyna and V. Pophristic, *J. Phys. Chem. B*, 2009, **113**, 7041; (*e*) Z. Liu, A. Teslja and V. Pophristic, *J. Comput. Chem.*, 2011, **32**, 1846; (*f*) S. Vemparala, I. Ivanov, V. Pophristic, K. Spiegel and M. L. Klein, *J. Comput. Chem.*, 2006, **27**, 693; (*g*) V. Pophristic, S. Vemparala, I. Ivanov, Z. Liu, M. L. Klein and W. F. DeGrado, *J. Phys. Chem. B*, 2006, **110**, 3517.
9 A. Laio and M. Parrinello, *Proc. Natl. Acad. Sci. U. S. A.*, 2002, **99**, 12562.
10 A. Pietropaolo and T. Nakano, *J. Am. Chem. Soc.*, 2013, **135**, 5509.
11 G. Diaz Leines and B. Ensing, *Phys. Rev. Lett.*, 2012, **109**, 020601.
12 T. Qi, V. Maurizot, H. Noguchi, T. Charoenraks, B. Kauffmann, M. Takafuji, H. Ihara and I. Huc, *Chem. Commun.*, 2012, **48**, 6337.
13 (*a*) D. Chakrabarti and D. J. Wales, *Soft Matter*, 2011, **7**, 2325; (*b*) P. Tao, J. R. Parquette and C. M. Hadad, *J. Chem. Theory Comput.*, 2012, **8**, 5137.

